CHAPTER 1

Extragalactic Radio Sources as a Piece of the Cosmological Jigsaw

Early on, extragalactic radio sources have pointed to a cosmologically evolving Universe. They were also an important piece of evidence for the existence of supermassive black holes, now thought to be a key component of galaxies. The observation that the power of radio sources increases with redshift, whereas the cosmological assembly of mass proceeds vice versa means that radio sources have their strongest impact in the early Universe. Our simulations suggest that radio sources heat hot halo gas, boost star formation in disc galaxies and other cold gas in the vicinity, possibly filaments, by a surround and squash mechanism. They might cause gaseous outflows in connection with stellar feedback. This might be an important mode of star formation for forming massive galaxies. Analysis of the jet-environment interaction may provide insights into black-hole physics and jet formation, e.g., rotational energy extraction (Blandford-Znajek) or how frequent black-hole binaries or multiple systems are. The former relates to fundamental questions about the nature of black holes. The latter is expected from hierarchical cosmology. Extragalactic radio sources thus continue to corroborate the cosmological picture and lead the way towards new, exciting discoveries.

1. Introduction

Extragalactic radio sources were first identified in the 1950s and very soon opened up a new perspective on the Universe (Norris , 2017, for a review). They were much more powerful than galaxies and the fact that they could be resolved with radio interferometers meant that they were bigger than galaxies, perhaps related to galaxy mergers (Baade & Minkowski , 1954). The first identified extragalactic radio source, Cygnus A (Fig. 1), was optically identified with a central member of a galaxy cluster (Baade & Minkowski , 1954). This proved to be no accident: Observationally, central cluster galaxies are frequently associated with powerful radio sources, especially if they have a dense and rapidly cooling intra-cluster medium (Burns , 1990). The dense gas is crucial to confine the radio emitting plasma, such that the observed high energy densities may be produced (e.g. Kaiser et al., 1997; Hardcastle & Krause, 2013). Powerful radio sources are hence observed in environments of enhanced galaxy density (Longair & Seldner , 1979). The somewhat weaker sources with complex morphology prefer richer environments than classical doubles. Such radio sources can heat the gas in their environment significantly, which is now believed to play a major role in keeping hot atmospheres of groups and clusters of galaxies hot (e.g., McCarthy et al. , 2008; Turner & Shabala , 2015),
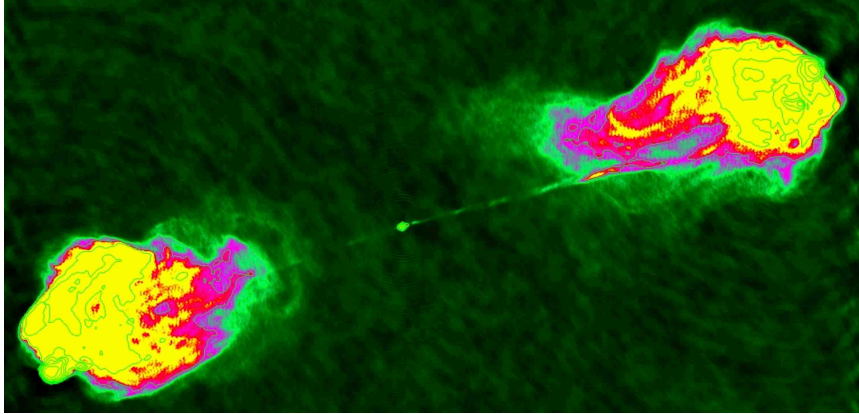
FIGURE 1. Very Large Array 5 GHz image of the first identified extragalactic radio source, Cygnus A (Carilli & Barthel, 1996). The colour scale was adjusted to emphasise the faint jets. Contours reveal the bright hotspots. The radio map was kindly provided by Chris Carilli and Rick Perley.

and thus impacts on cooling of hot gas, gas inflow and star-formation in massive galaxies (Croton et al., 2006).

By the end of the 1950s, catalogues of radio sources became available (2C, 3C, Sidney 85 MHz). The source counts ruled out a steady-state Universe and clearly favoured big-bang cosmology (Norris , 2017). The important result reflected the fact that radio sources become more powerful with redshift. The most powerful radio sources are found at cosmological redshifts (e.g., Carilli et al. , 2001, Fig 2). Because the assembly of galaxies and galaxy clusters proceeds hierarchically, bottom up, this means that radio sources must have had an enormous impact at high redshift. Powerful double radio sources like Cygnus A have an energy budget of the order of 10^{62} erg (Krause, 2005). A reasonable fraction of this energy is transfered to the ambient gas (Hardcastle & Krause, 2013). While this is only a few per cent of the binding energy of the intracluster medium in the nearby host galaxy cluster of Cygnus A, it may be similar to or even exceed the values for a high redshift environment. This is in line with expectations for "pre-heating" of galaxy clusters (McCarthy et al. , 2008), and may terminate star formation in the Megaparsec scale environment (Rawlings & Jarvis, 2004).

High quality, high resolution radio maps became available with the Very Large Array (VLA) and very long baseline interferometry (VLBI). They showed clear detections of the jets, collimated, relativistic plasma beams that connect the energy generation region around the supermassive black holes to the sometimes Megaparsec-scale radio lobes (Fig. 1). Such a mechanism had been proposed before, because of the huge energy requirements to power the lobes (Blandford & Rees, 1974; Scheuer, 1974). This gave important support to supermassive black hole hypothesis and was a striking example that properties of large-scale radio sources can be used to constrain the central engine.

Here I would like to review some main points on what we have learnt from radio sources so far in the context of heating of intracluster gas, impact at high redshift and the central engine.
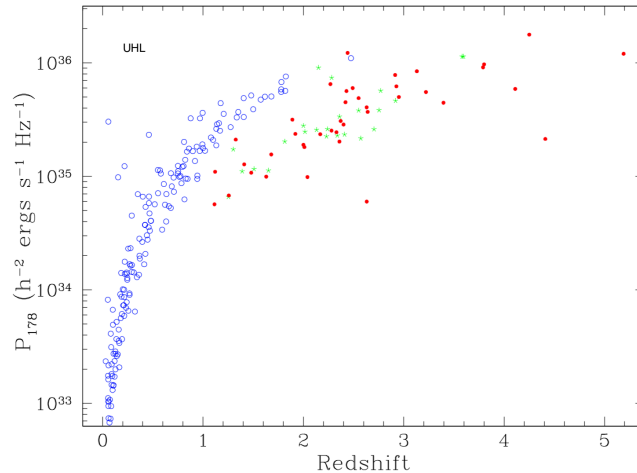
FIGURE 2. Radio power at a rest-frame frequency of 178 MHz versus redshift for the 3C sample (open circles) and fainter samples (filled circles and stars), adopted from Carilli et al. (2001).

2. Heating of the intracluster medium

Galaxy clusters are filled with hot gas with temperatures in excess of 1 keV (Böhringer & Werner, 2010, for a recent review). A significant fraction of galaxy clusters has cooling times in their core that are shorter than the Hubble time (cool core clusters), which is now thought to be offset by heating via thermal conduction and energy input by intermittent radio source production in the central dominant (CD) galaxy of the cluster (McNamara & Nulsen, 2007; Fabian, 2012; Turner & Shabala , 2015, Fig. 3). We first review basic radio source physics and will discuss different modes of heating from this perspective.

2.1. Basic radio source physics. Differential rotation in accretion flows on to a black hole will shear and amplify the magnetic field in the direction of rotation. This builds up magnetic pressure which can drive an outflow along the spin axis (Pudritz et al., 2012, for a recent review). The toroidal magnetic field will at the same time accelerate and collimate the outflow to a finite opening angle. Simulations have produced half opening angles of $3-7°$ for the case of geometrically thin Keplerian accretion discs (e.g., Porth & Fendt, 2010). General relativistic simulations of jet formation from geometrically thick accretion tori show somewhat wider jets. For example, Beckwith et al. (2009) find about $20°$. The magnetic field drops strongly outwards, away from the jet formation region while the kinetic energy increases (Pudritz et al., 2012), dominating after a few tens of Schwarzschild radii (Porth & Fendt, 2010).

Because of the still finite opening angle, the ram pressure in the jet now drops as r^{-2}, r being the distance to the black hole. The jet can recollimate hydrodynamically to zero opening angle, when the sideways ram pressure has dropped to the level of the ambient pressure. Krause et al. (2012) show for a constant ambient gas distribution that this depends solely on the half-opening angle of the initially conical jet (see also Fig 4):
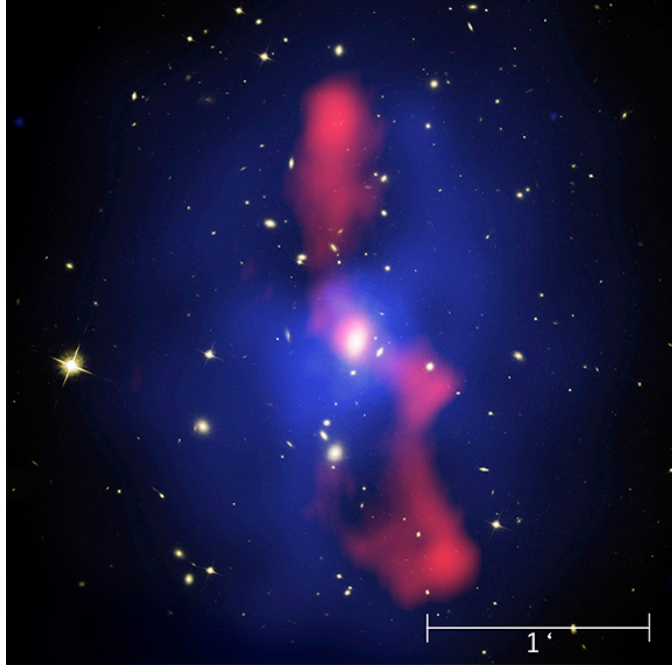
FIGURE 3. Galaxy cluster MS0735.6+7421. White: optical (Hubble), blue: X-ray (Chandra), red: 330 MHz radio image. The central, biggest galaxy in the cluster produces the radio source, which has displaced the X-ray gas, carving out cavities. Credit: X-ray: NASA/CXC/Univ. Waterloo/B.McNamara; Optical: NASA/ESA/STScI/Univ. Waterloo/B.McNamara; Radio: NRAO/Ohio Univ./L.Birzan et al. (compare also McNamara & Nulsen, 2007).

If it is less than $24°$, the jet will collimate hydrodynamically at a length scale L_{1a}, which, for a jet at half the speed of light, a half-opening angle of $5°$, jet power Q_0 and ambient pressure p_x is given by:

$$(1) \qquad L_{1a} = 3 \, \text{kpc} \left(\frac{Q_0}{10^{45} \, \text{erg s}^{-1}} \right)^{1/2} \left(\frac{p_x}{10^{-9} \, \text{dyn cm}^{-3}} \right)^{-1/2} .$$

The jet then also becomes underdense with respect to its environment and forms a cocoon of shocked jet material around the jet, which will often provide the pressure for the hydrodynamic recollimation. The jet lobe system then expands self-similarly, length scales expanding as (t: time, ambient density: $\rho_0(r/r_0)^\kappa$):

$$(2) \qquad L \propto \left(\frac{Q_0 t^3}{\rho_0} \right)^{\frac{1}{\kappa+5}}$$

(Kaiser & Alexander, 1997; Krause, 2003), until the lobes reach pressure equilibrium with the environment (Hardcastle & Krause, 2013). The source can however continue expanding as long as the jet is active.

If the half-opening angle is greater than $24°$, then the jet cannot recollimate before the hotspot stalls because the forward ram pressure is matched by the ambient

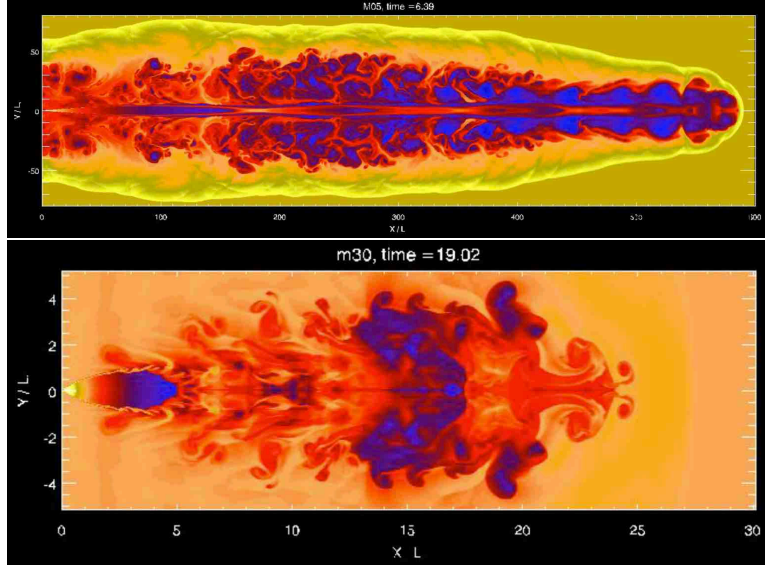FIGURE 4. Hydrodynamic simulations of jets with different opening angles. Top: With a half-opening angle of $5°$, jets may collimate hydrodynamically. They stay supersonic up to the tip of the cocoon, and may drive their terminal hotspots to infinity as long as the black hole remains active. Bottom: Jet with a half-opening angle of $30°$. The jet cannot collimate. Instead the terminal hotspot stalls where the jet's ram pressure equals the ambient pressure. Downstream, a transsonic, strongly entraining flow evolves.

pressure. Such sources will have a strong shock near

$$(3) \qquad L_{1c} = 2\,\mathrm{kpc} \left(\frac{Q_0}{10^{43}\,\mathrm{erg\,s^{-1}}} \right)^{1/2} \left(\frac{p_x}{10^{-11}\,\mathrm{dyn\,cm^{-3}}} \right)^{-1/2},$$

where we have now assumed a half-opening angle of $30°$. The flow will then evolve transsonically, entraining significant amounts of ambient material.

Krause et al. (2012) have proposed that these two basic radio source morphologies may explain the observed Fanaroff-Riley (FR) dichotomy. Jets with wide opening angle would produce the centre-bright FR I radio sources, whereas jets with narrow opening angles would form the edge-brightened FR IIs. Other FR I models have been proposed, based on instabilities (e.g., Kaiser & Best, 2007), expansion of overpressured jets (Perucho & Martí, 2007), and entrainment of stellar winds (Komissarov, 1994).

When the pressure of the lobes approaches the ambient pressure, the lobes start to detach from each other and the ambient gas refills the centre of the cavity (Fig. 5).

2.2. Modes of heating. Irreversible heat transfer is conveniently measured by the entropy index $s = kTn^{-2/3}$, which is constant under adiabatic changes, but increases in shocks and by viscous dissipation.

2.2.1. *Strong shocks.* The most obvious heat source for intracluster gas is the leading bow shock of a radio source. Strong shocks are usually not seen in observed
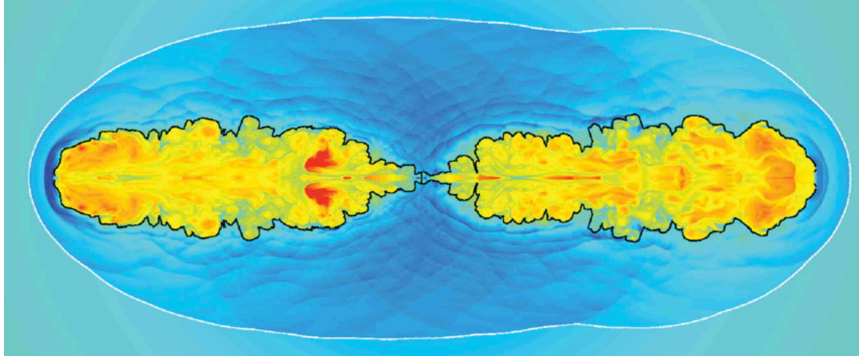
FIGURE 5. Simulation of the interaction of a radio lobe with dense intracluster medium, adopted from Hardcastle & Krause (2013). The outer bow shock is seen as a white line, the contact surface that separates the shocked ambient gas from the shocked jet gas in the cocoon / radio lobe is shown as a black line. The lobes have started to detach from the central region, allowing ambient gas to refill the cavity. Ripples are seen in the shocked ambient gas due to motion of the contact surface due to the turbulent motions in the cocoon / radio lobe region.

sources, as expected from radio source models: Since the Mach number of the bow shock quickly declines, the observation only implies that radio sources tend to live much longer than they need to get to pressure equilibrium. Only the innermost regions of a cluster will then be efficiently heated by the shock, and much of the energy is not used for heating the cluster gas. The simulations of Hardcastle & Krause (2013) illustrate this process (Fig. 5). The simulated radio source heats the central 50 kpc very efficiently. Because of this, that gas is buoyantly uplifted and the region is refilled with gas with only 10-20 per cent higher entropy index. To prevent significant cooling in this way, the radio source must be active recurrently. Observations find the rising bubbles left-over in the X-ray gas (e.g., Fabian, 2012). So this may indeed be a mode that is frequently realised in nature.

2.2.2. *Weak shocks / ripples.* A similar faction of the energy in a radio source is stored in lobes and, respectively, ambient gas (e.g. Hardcastle & Krause, 2013; English et al., 2016). About half of the lobe energy is accounted for by turbulent motions. The random motions disturb the contact surface between radio lobes and intracluster medium and run weak shock waves or ripples into the part of the intracluster medium that has already been shocked by the leading bow shock (Fig. 5). Such ripples are observed in some galaxy clusters and may carry enough energy to offset cooling in the cluster (Fabian, 2012). The observed sources suggest that the perturbations of the contact surfaces are enhanced by intermittency of the radio source or, perhaps, precession (more below). Viscous dissipation of such ripples could heat the intracluster gas to larger radii than the strong shocks.

3. High redshift radio sources

High redshift radio sources (HZRGs, redshift $z > 1$) can be more powerful than their low redshift counterparts and are associated with larger emission line lobes and very high rates of star formation (Miley & De Breuck, 2008, for a review). Most
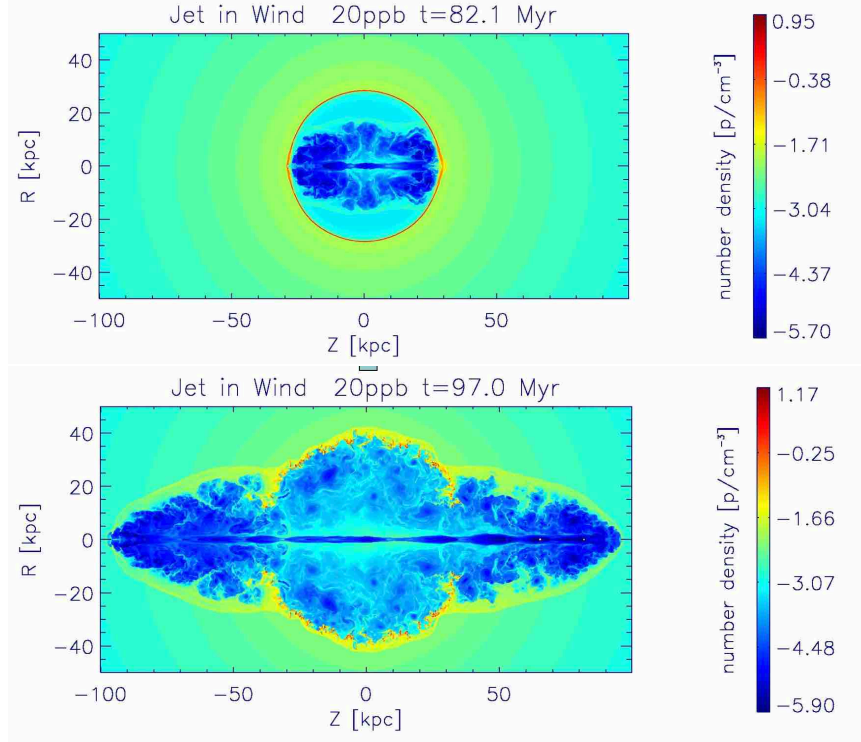
FIGURE 6. Hydrodynamic simulations of a jet in a galactic wind shell (Krause, 2005). The jet is efficiently trapped by the wind shell until the radio lobe fills the shell region. The shell is then accelerated and fragmented by the Rayleigh-Taylor instability. This may explain Lyman α self-absorption in high redshift radio galaxies.

HZRGs live in so-called proto-clusters, regions of several times $10^{14} M_\odot$ that are not virialised yet, but are thought to evolve into big clusters of galaxies by redshift zero (Venemans et al., 2007). The space density of galaxy clusters at redshift zero is compatible with the idea that all clusters had such a powerful radio source when they where assembled (McLure & Dunlop, 2001). HZRGs hence highlight the early stages of galaxy clusters and at the same time are laboratories for feedback in massive galaxies when they have not yet transformed into red ellipticals with little star formation.

3.1. Lyman α haloes. HZRG are frequently associated with emission line haloes with sizes up to 100 kpc (Miley & De Breuck, 2008). High fidelity radio images of HZRGs are not yet available, but the halos are aligned in direction with the radio sources and may thus correspond to the region occupied by the radio lobes. They evidence massive gaseous outflows with turbulent and bulk outflow velocities of the order of a few hundred km/s (Nesvadba et al., 2017). While energetically feasible, it remains unclear if the radio source is solely responsible for these outflows. In hydrodynamic simulations of the interaction of jets with clumpy, dense interstellar medium in the host galaxies, Mukherjee et al. (2016) find efficient energy transfer, but only for as long as the jet is contained in the galaxy,
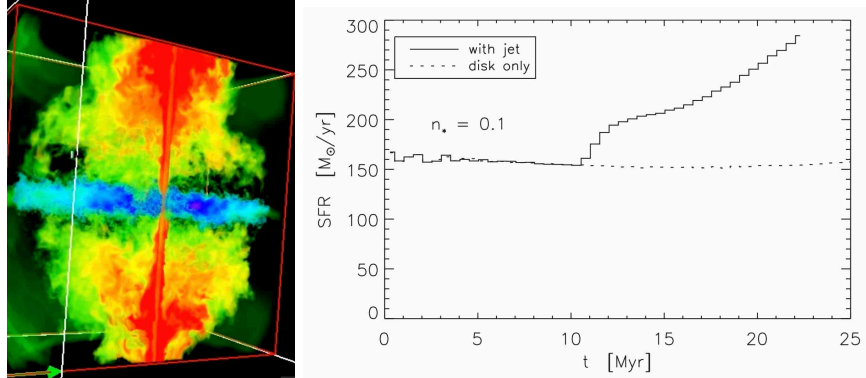
FIGURE 7. Hydrodynamic simulations of jet induced star formation in a massive high redshift galaxy (Gaibler et al., 2012). The radio lobes surround the interstellar medium and squash it by their high pressure. This enhances the star formation rate significantly.

which is too short to produce the large-scale outflows. In multi-phase turbulence simulations, Krause & Alexander (2007) show that the turbulence of the radio plasma in jet cocoons could accelerate entrained emission line gas to the observed velocities. It is well possible that early jet and also stellar feedback play a crucial role in launching the gas off the galaxy with cocoon turbulence taking over on larger scales.

3.2. Lyman α self-absorption. Lyman α emission from HZRG is frequently self-absorbed within typically a few hundred km/s bluewards of the emission peak (Miley & De Breuck, 2008; Swinbank et al., 2015). The best explanation is an expanding, radiative shell in the snow-plough phase (Krause, 2005). The shell cannot be driven by the radio source, because it would then be too fast, probably would not cool enough to form neutral hydrogen, and, if it would, its Ly α luminosity would violate observational limits. The shell is therefore likely driven by the stellar feedback in the strongly star-forming hosts. It sweeps up the hot atmosphere of its host galaxy, likely transforming it to stars. This might be a significant channel of forming globular clusters directly in the halo of a galaxy (Krause, 2002). The wind shells are disrupted by the radio sources (Krause, 2005, Fig 6)

3.3. Jet-induced star formation and galaxy transformation. Powerful HZRGs provide excess pressure over a period of at least tens of Myr. This may further compress any dense clouds affected by the radio lobes, in particular in the host galaxy and enhance the star formation rate. We have tested this quantitatively in hydrodynamic simulations (Gaibler et al., 2012, Fig 7), finding about a factor of two increase. Subsequent instabilities may enhance the star formation rate over an even longer timescale (Bieri et al., 2016). This raises the question, if radio source activated, boosted star formation is preferentially picked up in observations at high redshift (Silk & Mamon, 2012).

The radio source thus transforms the host galaxy in three ways: Firstly, the gas in the galaxy is used up much faster than without the radio source. Secondly, any dense gas around the galaxy (e.g., cold streams or wind shells) will suffer the same fate. Thirdly, the hot gas that has not been swept up previously by star-formation

driven winds will now be heated to the multi-keV regime, increasing its cooling time by orders of magnitude. Such a galaxy must, no doubt, quickly become a red and dead elliptical.

4. The central engines

4.1. Rotational energy extraction and jet composition. Jets carry properties of the central engine out to large scales, where they may be observed with comparative ease. Energy, momentum and mass flux, plasma composition and the large-scale electric current through the jet-lobe system (Gaibler et al., 2009) are conserved quantities which characterise the processes in the direct vicinity of supermassive black holes. For example, modelling the jet power in MS0735.6+7421 (Fig. 3) and comparing with the likely accretion power of the supermassive black hole in the host galaxy, McNamara et al. (2009) proposed that the radio source may be powered by extraction of rotational energy of the supermassive black hole (Blandford & Znajek, 1977). This is one of the motivations to model the kinetic power. For a given jet power, the observed radio luminosity depends on the environment (e.g., Hardcastle & Krause, 2013, 2014; English et al., 2016). Radio fluxes, sizes and spectra, in combination with X-ray data for the environment or, in the absence of the latter, optical magnitudes of the host galaxies as a proxy, allow to model composition and kinetic power of individual radio sources in detail. We have recently applied such techniques to a sample of powerful FR II radio sources (Turner et al., 2018, 2017). The distribution of jet powers extends up to about 10^{47} erg/s, the Eddington luminosity of a $10^9 M_\odot$ black hole. Hence, there is currently no evidence of spin powering for this population. Further, our results are consistent with pure electron-positron plasma in the radio lobes. In this context, it is interesting to note that the 511 keV electron-positron annihilation feature has recently been directly observed in a jet production event of a galactic, stellar mass black hole (Siegert et al., 2016, Fig. 8). Past jet production of the Milky Way's supermassive black hole, Sgr A*, of which the Fermi bubbles may be evidence of, may have contributed to the Galactic positron reservoir (Siegert et al., 2016).

4.2. Binary supermassive black holes. Extragalactic radio sources are ideally suited to track binarity in supermassive black holes (Begelman et al., 1980). After a galaxy merger, the two supermassive black holes are expected to quickly approach each other to sub-parsec separation (Mayer, 2017). The black hole spins will then precess around the orbital angular momentum vector with the geodetic period:

$$(4) \qquad P_{\mathrm{gp}} = 41 \, \mathrm{Myr} \, d_{\mathrm{pc}}^{5/2} M_9^{-3/2} r^{-1} (4 - r)^{-1} \, ,$$

where d_{pc} is the separation in pc, M_9 is the total black hole mass in $10^9 M_\odot$, and r is the mass ratio of the two black holes. The timescale is comparable to the age of extended radio sources, and hence, if the jet is emitted along the spin axis of one black hole, it's precession might be observable. Associated orbital timescales of the order of tens or hundreds of years are accessible to VLBI multi-epoch observations.

There is indeed plenty of evidence for precession in radio sources (Krause et al. in prep.). The perhaps best studied example, Cygnus A shows point-reflection symmetry, the jet is not identical with the lobe axis, and the direction of jet and counterjet differ by 178°, difficult to explain in a standard jet plus counterjet scenario or by jet-cloud interactions, but perhaps expected from relativistic aberration
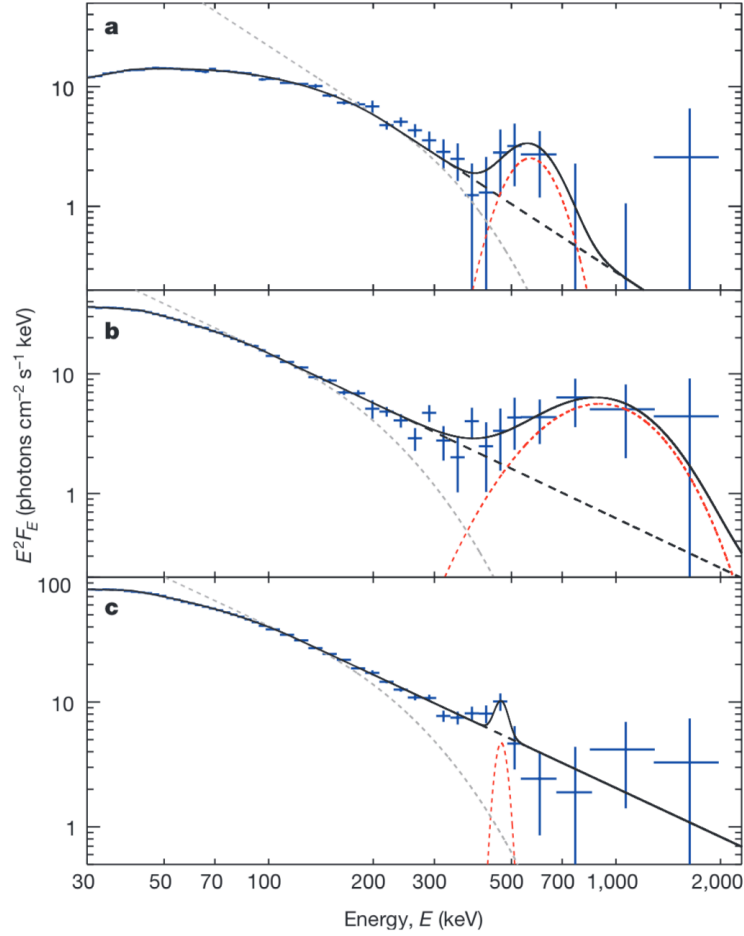
FIGURE 8. Evidence for electron-positron plasma from the galactic, jet-producing stellar mass black hole in V404 Cygni (Siegert et al., 2016). A broad annihilation line with variable width has been detected with the gamma ray spectrometer onboard INTEGRAL.

in precessing jets (Gower et al., 1982). The geometry is consistent with a precession period of $\approx 10^6$ yr, which can be explained by a binary supermassive black hole with less than 0.5 pc separation (Krause et al. in prep.). The VLBI jet has a helical structure (Boccardi et al., 2016) which can be explained by orbital motion of a binary with about 0.05 pc separation, consistent with the large-scale analysis.

We analysed a complete sample of radio sources (Krause et al. in prep.). Point symmetry, relativistic aberration ring-like hotspots and other features relating to precession are frequently seen. We find good evidence for precession in 73 per cent of the 33 sources.

Complementary evidence for binary black holes in jet sources is also very strong. For example, Lister et al. (2013) show that VLBI jets commonly change their position angle in time, some show periodic changes, as expected from orbital motion in a jet-producing binary.
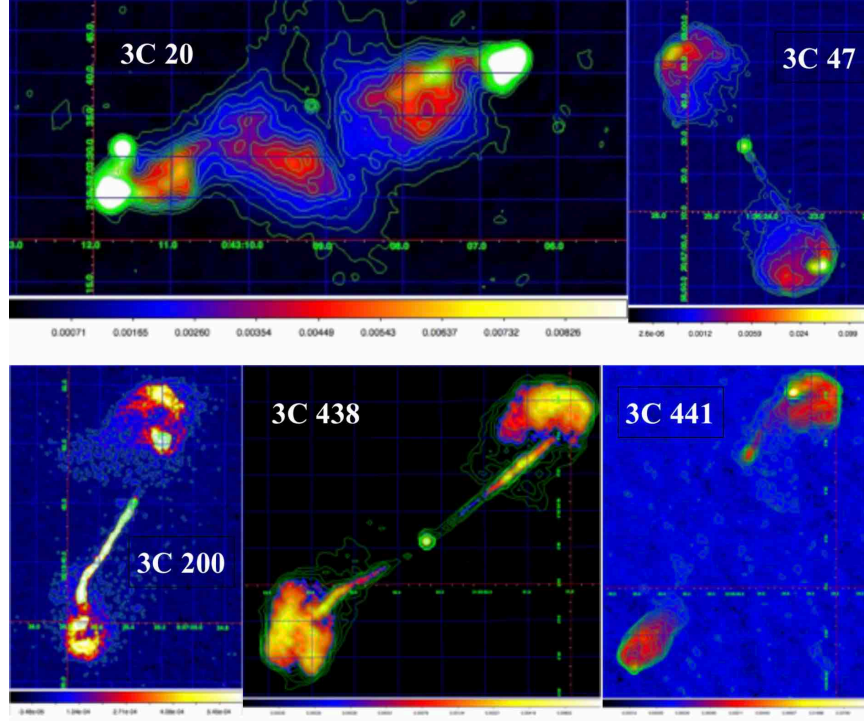
FIGURE 9. VLA radio maps of radio sources with strong evidence for jet precession.

These findings strongly suggest that powerful extragalactic radio sources may point to close binary supermassive black holes, with implications for the cosmological history of black hole merging and gravitational wave experiments.

Bibliography

Baade, W., & Minkowski, R. 1954, ApJ, 119, 206

Beckwith, K., Hawley, J. F., & Krolik, J. H. 2009, ApJ, 707, 428

Begelman, M. C., Blandford, R. D., & Rees, M. J. 1980, Nature, 287, 307

Bieri, R., Dubois, Y., Silk, J., Mamon, G. A., & Gaibler, V. 2016, MNRAS, 455, 4166

Blandford, R. D., & Rees, M. J. 1974, MNRAS, 169, 395

Blandford, R. D., & Znajek, R. L. 1977, MNRAS, 179, 433

Boccardi, B., Krichbaum, T. P., Bach, U., et al. 2016, Astronomy & Astrophysics, 585, A33

Böhringer, H., & Werner, N. 2010, Astronomy & Astrophysics Review, 18, 127

Burns, J. O. 1990, AJ, 99, 14

Carilli, C. L., & Barthel, P. D. 1996, Astronomy & Astrophysics Review, 7, 1

Carilli, C. L., Miley, G., Röttgering, H. J. A., et al. 2001, Gas and Galaxy Evolution, 240, 101

Croton, D. J., Springel, V., White, S. D. M., et al. 2006, MNRAS, 365, 11

English, W., Hardcastle, M. J., & Krause, M. G. H. 2016, MNRAS, 461, 2025

Fabian, A. C. 2012, Annu. Rev. Astron. & Astrophys., 50, 455

Gaibler, V., Krause, M., & Camenzind, M. 2009, MNRAS, 400, 1785

Gaibler, V., Khochfar, S., Krause, M., & Silk, J. 2012, MNRAS, 425, 438

Gower, A. C., Gregory, P. C., Unruh, W. G., & Hutchings, J. B. 1982, ApJ, 262, 478

Hardcastle, M. J., & Krause, M. G. H. 2013, MNRAS, 430, 174

Hardcastle, M. J., & Krause, M. G. H. 2014, MNRAS, 443, 1482

Kaiser, C. R., & Alexander, P. 1997, MNRAS, 286, 215

Kaiser, C. R., Dennett-Thorpe, J., & Alexander, P. 1997, MNRAS, 292, 723

Kaiser, C. R., & Best, P. N. 2007, MNRAS, 381, 1548

Komissarov, S. S. 1994, MNRAS, 269, 394

Krause, M. 2002, Astronomy & Astrophysics, 386, L1

Krause, M. 2003, Astronomy & Astrophysics, 398, 113

Krause, M. 2005, Astronomy & Astrophysics, 431, 45

Krause, M. 2005, Astronomy & Astrophysics, 436, 845

Krause, M., & Alexander, P. 2007, MNRAS, 376, 465

Krause, M., Alexander, P., Riley, J., & Hopton, D. 2012, MNRAS, 427, 3196

Lister, M. L., Aller, M. F., Aller, H. D., et al. 2013, AJ, 146, 120

Mayer, L. 2017, Journal of Physics Conference Series, 840, 012025

McCarthy, I. G., Babul, A., Bower, R. G., & Balogh, M. L. 2008, MNRAS, 386, 1309

McLure, R. J., & Dunlop, J. S. 2001, MNRAS, 321, 515

McNamara, B. R., & Nulsen, P. E. J. 2007, Annu. Rev. Astron. & Astrophys., 45, 117

McNamara, B. R., Kazemzadeh, F., Rafferty, D. A., et al. 2009, ApJ, 698, 594

Miley, G., & De Breuck, C. 2008, Astronomy & Astrophysics Review, 15, 67

Mukherjee, D., Bicknell, G. V., Sutherland, R., & Wagner, A. 2016, MNRAS, 461, 967

Nesvadba, N. P. H., De Breuck, C., Lehnert, M. D., Best, P. N., & Collet, C. 2017, Astronomy & Astrophysics, 599, A123

Longair, M. S., & Seldner, M. 1979, MNRAS, 189, 433

Norris, R. P. 2017, Nature Astronomy, 1, 671

Perucho, M., & Martí, J. M. 2007, MNRAS, 382, 526

Porth, O., & Fendt, C. 2010, ApJ, 709, 1100

Pudritz, R. E., Hardcastle, M. J., & Gabuzda, D. C. 2012, Space Sci. Rev., 169, 27

Rawlings, S., & Jarvis, M. J. 2004, MNRAS, 355, L9

Scheuer, P. A. G. 1974, MNRAS, 166, 513

Siegert, T., Diehl, R., Greiner, J., et al. 2016, Nature, 531, 341

Siegert, T., Diehl, R., Khachatryan, G., et al. 2016, Astronomy & Astrophysics, 586, A84

Silk, J., & Mamon, G. A. 2012, Research in Astronomy and Astrophysics, 12, 917

Swinbank, A. M., Vernet, J. D. R., Smail, I., et al. 2015, MNRAS, 449, 1298

Turner, R. J., & Shabala, S. S. 2015, ApJ, 806, 59

Turner, R. J., Rogers, J. G., Shabala, S. S., & Krause, M. G. H. 2018, MNRAS, 473, 4179

Turner, R. J., Shabala, S. S., & Krause, M. G. H. 2017, arXiv:1711.04600

Venemans, B. P., Röttgering, H. J. A., Miley, G. K., et al. 2007, Astronomy & Astrophysics, 461, 823